PERGAMON

Journal of Structural Geology 25 (2003) 1445–1450

JOURNAL OF STRUCTURAL GEOLOGY

www.elsevier.com/locate/jsg

The effect of décollement dip on geometry and kinematics of model accretionary wedges

Hemin A. Koyi[a,*], Bruno C. Vendeville[b]

[a]*Hans Ramberg Tectonic Laboratory, Department of Earth Sciences, Uppsala University, Uppsala, Sweden*
[b]*Bureau of Economic Geology, University of Texas at Austin, Austin, TX, USA*

Received 24 February 2002; received in revised form 1 November 2002; accepted 26 November 2002

Abstract

We conducted a series of sand-box models shortened asymmetrically above a frictional-plastic décollement to study the influence of amount and sense of the décollement dip on the geometry and kinematics of accretionary wedges. Model results illustrate that the amount and direction of décollement dip strongly influence the geometry and mode of deformation of the resulting wedge. In general, for models having similar décollement frictional parameters, the resulting wedge is steeper, grows higher and is shorter when shortened above a décollement that dips toward the hinterland. At 42% bulk shortening, the length/height ratio of wedges formed above a 5°-dipping décollement was equal to 2.4 whereas this ratio was equal to 3 for wedges shortened above a horizontal décollement. Moreover, models with a hinterland dipping décollement undergo larger amounts of layer parallel compaction (LPC) and area loss than models shortened above a non-dipping décollement. The effect of décollement dip on wedge deformation is most pronounced when basal friction is relatively high ($\mu_b = 0.55$), whereas its effect is less significant in models where the basal décollement has a lower friction ($\mu_b = 0.37$). Model results also show that increasing basal slope has a similar effect to that of increasing basal friction; the wedge grows taller and its critical taper steepens.

Keywords: Accretionary wedges; Sand-box models; Décollement dip; Basal friction

1. Introduction

Most accretionary wedges and fold-and-thrust belts form above a décollement dipping toward the hinterland. Although the dip of these décollements may increase as loading by growing wedge increases, recent work by Mariotti and Doglioni (2000) suggests décollement dips commonly vary from 1–5°; as in the western and northern Alps, to as much as 10–20°; as in the Apennines. In the front of the wedge, the regional dip of the basal décollement in western Taiwan is reasonably well constrained by seismic-reflection and deep-drilling data, as well as by cross-section restoration (Suppe and Namson, 1979; Suppe, 1980a,b; Namson, 1982). A décollement dip of 6° is believed to exist under the entire width of at least northern Taiwan. Because they control the deformation style and the wedge taper, the décollement dip and basal friction can be used to estimate the coefficient of internal friction within accretionary wedges (Davis et al., 1983). Davis et al. (1983) presented theoretical critical wedge profiles above dipping décollements and concluded that the taper was strongly controlled by the coefficient of internal friction of the wedge. Antiformal stacks in the Sulaiman fold belt in Pakistan are interpreted to have formed in response to shortening of a Triassic-to-Recent sedimentary cover above a 2.5°-dipping basal detachment (Jadoon et al., 1992).

Using an analytical approach, Davis et al. (1983) and Dahlen et al. (1984), applied a critical-taper model to natural and sand-box contractional wedges above hinterland-dipping décollements. The effect of basal friction on the geometry of accretionary wedges in nature (Davis and Engelder, 1985; Cotton and Koyi, 2000) and sand-box models (Colletta et al., 1991; Liu et al., 1992; Mulugeta and Koyi, 1992; Willett, 1992; Gutscher et al., 1996) has subsequently been studied by many workers who similarly employed critically tapered wedge model. These previous studies have concluded that higher basal friction leads to formation of a wedge having a higher taper (surface slope), whereas low basal friction leads to formation of a wedge

* Corresponding author. Tel.: +46-18-471-25-63; Fax: +46-18-471-25-91.
E-mail address: hemin.koyi@geo.uu.se (H.A. Koyi).

0191-8141/03/$ - see front matter © 2003 Elsevier Science Ltd. All rights reserved.
PII: S0191-8141(02)00202-X

having a gentler taper. In this study, we use results from physical models to illustrate the combined influences of varying the décollement dip and the basal friction onto the kinematics of accretionary wedges and fold-and-thrust belts.

2. Experimental procedure

The geometry and kinematics of a contractional wedge are directly related to the rheological properties of the accreted material, the basal friction and the décollement dip (e.g. Davis et al., 1983; Liu et al., 1992; Mulugeta and Koyi, 1992). In the six models presented here, we used the same type of dry quartz sand for all experiments, but varied the décollement dip and friction (Fig. 1). The models were identical, except for the coefficient of internal friction of the décollement and the amount and sense of the slope of the basal décollement, which were changed systematically between experiments. The series of models was divided into two subsets; in one set (three models) the model rested above a low-friction décollement of glass microbeads ($\mu_b = 0.37$); in a second set (three models) the model rested above a relatively high-friction décollement of sand ($\mu_b = 0.55$). In each set, one model was deformed above a horizontal décollement, a second model above a décollement dipping 5° toward the hinterland, and a third model was shortened above a décollement dipping 5° toward the foreland. Although models having foreland-dipping décollements correspond to less likely geological settings in nature, we conducted such models to better characterize the change in structural pattern when varying the basal slope across a wide range. In our models, we assume that the direction of the décollement dip is parallel to that of the foreland dip. Unlike in nature, where the dip of foreland typically increases toward the interior of the belt (von Huene, 1986), the décollement dip in experiments remained constant in each model, but changed between models. Erosion and sedimentation, likely to occur in nature, were not included in the models' design.

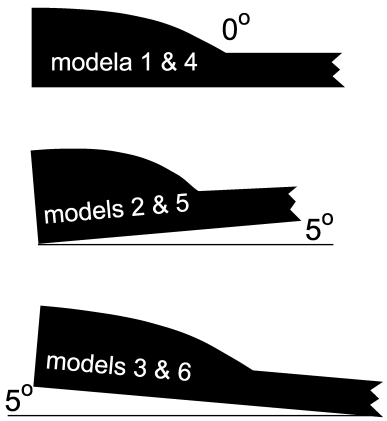

Fig. 1. Schematic illustration of décollement geometries used in this study. Models 1–3 used high-friction sand as the décollement material, whereas models 4–6 used low friction glass beads as the décollement material.

In each model the cover comprised a passive sand layer having various colors but identical rheological properties. The cover was initially 10 mm thick, 30 cm wide and 48 cm long and was then deformed asymmetrically by a rigid backstop (Fig. 2). The evolution of each model was recorded by time-lapse overhead photographs. The height and length of the resulting wedge were measured after every step of additional 1 cm shortening. The height was measured as the distance between the top of the décollement and the top of the cover where the wedge was highest. Along the strike direction, measurements were taken in the center, away from the model's lateral wall to avoid the influence of potential edge effects. All models were shortened between 40 and 48%, after which each model was buried under a layer of post-tectonic white sand in order to preserve its topography, then the model was hardened by spraying water to allow for serial sectioning and photographing (Fig. 2).

3. Scaling

Model results are applicable to their prototype if they are dynamically and kinematically scaled with respect to their natural counterparts. In our models the length ratio was 5×10^{-6} where 1 km in nature is simulated by 2 mm in the model (Table 1). Kinematic similarity was fulfilled for each model assuming that the sedimentary units in the prototype were similar to the sand layers, shortened above a dipping décollement. For a model to fulfil dynamic similarity with its prototype, a set of dimensionless ratios, which relate to physical properties of model materials and natural rocks, should be similar. We assumed that the material forming the wedge in nature is isotropic and obeys a Mohr–Coulomb behavior typical of that of most rocks in the upper continental crust. Well-sorted, well-rounded, dry quartz sand, which is a Coulomb material, was used as the model material because it has an angle of internal friction of about 0.7, similar to that of natural rocks in the upper 10 km of the continental crust (Hubbert, 1937; Vendeville et al., 1987; Koyi and Petersen, 1993; Weijermars et al., 1993). Cohesion, having the dimensions of stress, can be scaled by calculating the stress ratio for gravity stresses, σ^*: as follows (also see Table 1):

$$(\tau_{\text{model}}/\tau_{\text{nature}}) = \sigma^* = (\rho^* l^* g^*), \quad (1)$$

where τ_{model} and τ_{nature} are the cohesion values in model and nature, respectively, ρ^* is the density ratio between model and prototype, l^* is the length ratio, and g^* is the ratio for gravity acceleration, here equal to unity. The shear strength of sedimentary rocks ranges between 1 and 10 MPa (Hoshino et al., 1972). For clastic sediments, we have chosen an average volumetric mass of about 2550 kg m^{-3}. Our sand had a volumetric mass of 1700 kg m^{-3}. Using these figures, the stress ratio, σ^*, is 3.33×10^{-6}, and the cohesion in the model must lie between 3.3 and 33 Pa.

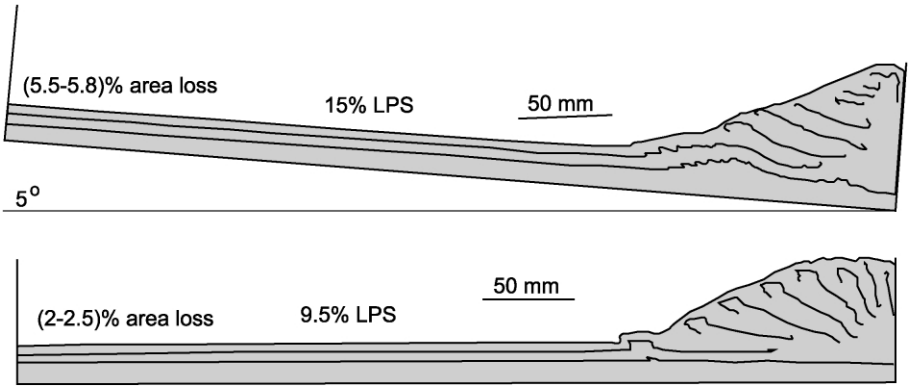

Fig. 2. Line drawing of two profiles of (A) a model shortened above a horizontal décollement and (B) a model shortened above a décollement dipping 5° toward the hinterland. The average of area loss and layer-parallel compaction shown here are measured from six profiles.

4. Model results and discussion

During the shortening all models formed a wedge of piggy-back imbricate stacks propagating forward in front of the rigid backstop (Fig. 3). The wedge grew in height and length as new imbricates formed in front by accreting undeformed sand. Wedges having different amounts of décollement-dip values or vergence, or basal friction had different geometry and propagation characteristics.

4.1. Wedge height versus length

Unlike in natural examples, measuring the height and length of a wedge during its evolutionary history is relatively easy in experiments. The wedge length can be measured directly on the model's surface, or measured on time-lapse overhead photographs. We measured the height of the wedges using a caliper located above the deforming model.

Previous modeling of loose sand shortened above a rigid substrate has shown that accretionary wedges do not grow self-similarly. Instead, the length and height of the model wedges increase disproportionately; the length of the wedge increases episodically when each new imbricate forms, while the wedge's height grows continually, first rapidly during the early stage of wedge formation, then much more slowly once the critical taper is reached (Koyi, 1995).

The results of the models presented here show that changing the amount and sense of a décollement dip influences the wedge growth, but that the slope's influence is less strong than that of changing the strength of the basal décollement. In models shortened above a high-friction décollement tilted 5° towards the hinterland, the wedge grew higher than in similar models having a horizontal décollement (Fig. 3a). The length of the wedge in these two models also increased differently. The wedge was shortest when forming above a décollement dipping 5° towards the hinterland. It was longer above a horizontal décollement and was longest above a décollement dipping 5° towards the foreland. The wedge's height was greatest above a décollement dipping 5° towards the hinterland, lower above a horizontal décollement, and lowest above a décollement dipping 5° towards the foreland. At 42% bulk shortening, the length/height ratio of wedges formed above a décollement dipping 5° towards the hinterland was equal to 2.4. This ratio was equal to 3 for wedges shortened above a horizontal décollement and 4 for wedges shortened above a décollement dipping 5° towards the foreland.

The influence of the basal slope on the wedge's height and length is less pronounced in models having a low-friction décollement. In these models, the 5°-hinterland slope of the décollement caused only a slight difference in height and length of the wedge (Fig. 3b). We infer that when basal friction is low, the role of basal slope is less important compared with other parameters, such as the angle of internal friction of the material forming the wedge itself. Consequently, changing the basal slope has less influence on the wedge's geometry and kinematics.

Comparison between two models with similar décollement dip, but different basal friction shows that the wedge in the model with high-basal friction grew taller than in the model with low-basal friction (Fig. 4a). In other words, the

Table 1
Scaling parameters between model and nature. Subscripts m and n denote model and nature, respectively

Quantity	Nature	Model	Scaling ratio
Acceleration due to gravity	9.81	9.81	$a_m/a_n = 1$
Thickness	1 km	5 mm	$l_m/l_n = 5 \times 10^{-6}$
Friction coefficient	0.85	0.73	0.86
$(\rho lg/\tau_0)$ ratio	10	5.6	0.56
Shortening rate	0.6–5 cm/yr	1.0×10^4 cm/yr	6×10^{-5}–5×10^{-4}

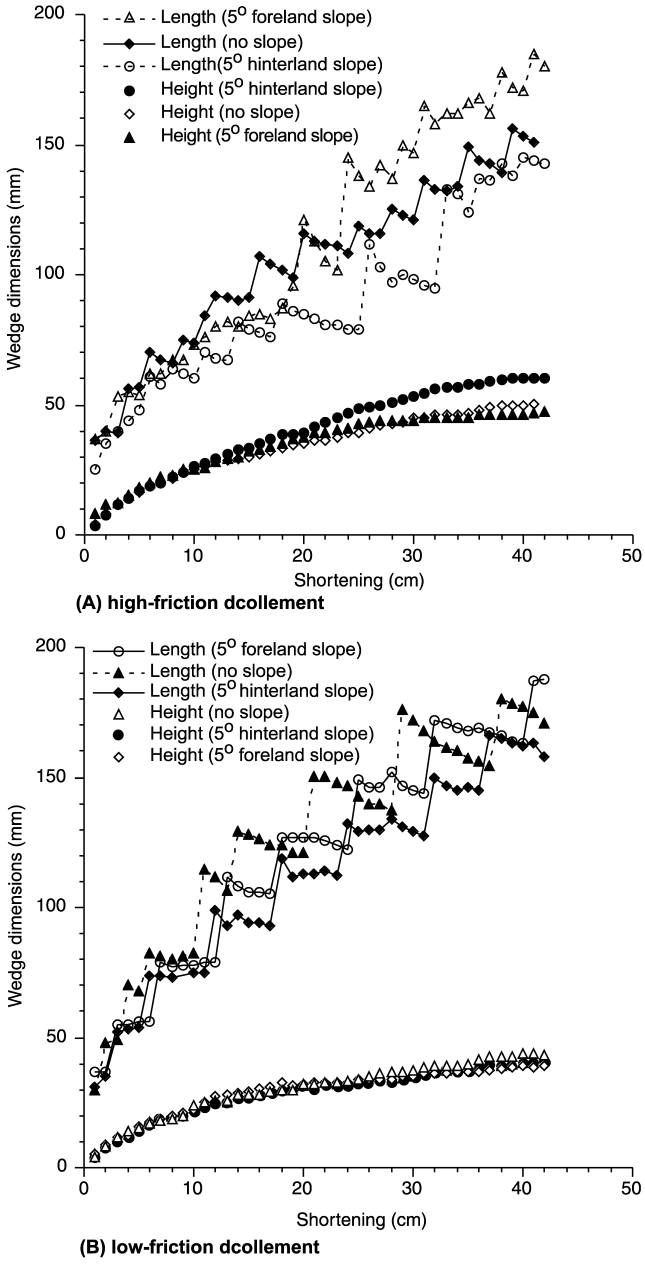

Fig. 3. Plots of wedge height and length for models shortened above (A) a high-friction décollement and (B) a low-friction décollement. Note that the difference in wedge height between models with two different slopes is less profound above low-friction décollements. Note also that there are fewer imbricates and that these imbricates form at more regular intervals above a low-friction décollement. Each step in the length curves represents the formation of a new imbricate.

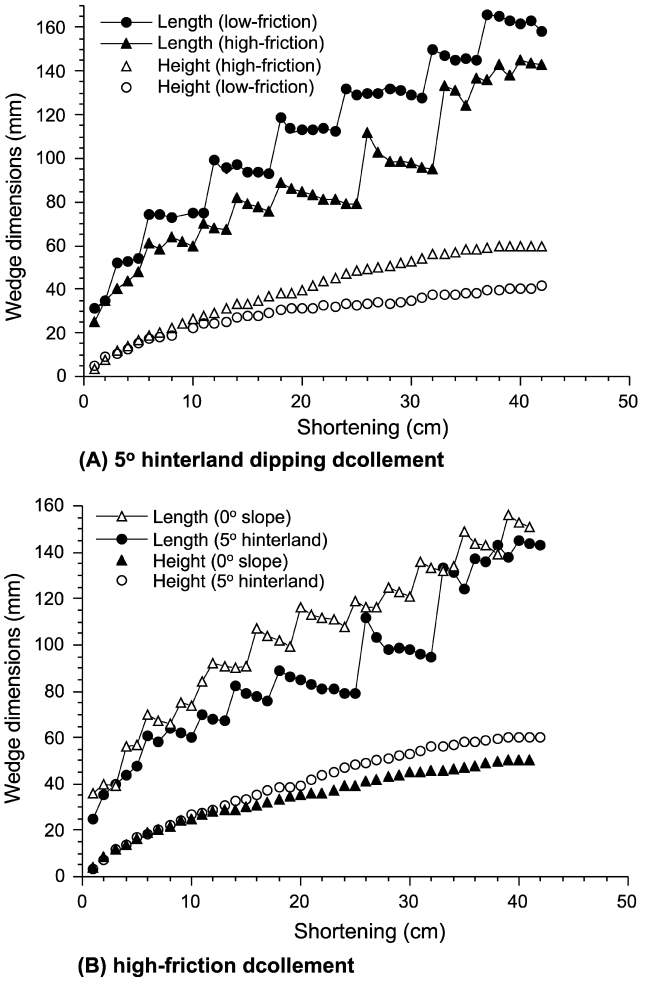

Fig. 4. (A) Plots of wedge height and length with shortening for two models shortened above a décollement dipping 5° toward the hinterland with different basal friction. Note that the wedge grows taller when basal friction is high, but is shorter. (B) Plots of wedge height and length with shortening for two models shortened above a high-friction décollement (one with zero slope and the other with 5° towards the hinterland). Above a non-dipping décollement, the resulting wedge is longer than above the 5°-dipping décollement.

effect of basal friction is far more significant than the effect of basal slope. As the décollement dip increases, the normal component of the applied stress increases, leading to an increase in the frictional stress along the décollement. However, if the basal friction is low, this increase in stress remains minor. Indeed, models shortened above a hinterland-dipping, low-friction décollement had a gentler taper than those above a horizontal, high-friction décollement (Fig. 4b). It is also interesting to note that in our models, the difference in the angle of internal friction between 'weak' and 'strong' décollement was approximately 10°, from 30° in sand to 20° in glass microbeads. In nature, fluid overpressure can alter the amount of basal friction much more drastically and is capable of reducing the strength of the décollement by 90% or more. Consequently, the impact of changing the friction by fluid pressure is likely to have an even greater impact than the influence of the slope.

The effect of basal friction on the geometry of an accretionary wedge has been modeled and discussed in detail by many workers (Davis and Engelder, 1985; Colletta et al., 1991; Liu et al., 1992; Willett, 1992; Cotton and Koyi, 2000; Koyi et al., 2000). However, its effect in connection with a dipping décollement has not been reported before. Previously, it has been shown that a wedge shortened above a high-friction décollement develops a steep taper, whereas wedges shortened above a low-friction décollement have a

lower taper. To compare this model result with a natural example, balanced sections (six sections in a sequence) of the antiformal stacks in the Sulaiman fold belt in Pakistan, prepared by Jadoon et al. (1992), were used to calculate the evolution of the height and length of a natural wedge. The cross-section was based on seismic reflection profiles, surface geology, borehole and landsat data (Jadoon et al., 1992). When measuring the height of the antiformal stacks from the sequential cross-sections, the eroded parts of the layers were added to the height of the anticlinal stacks. This was done by assuming that the layers had a constant thickness in the sections. This assumption may give a maximum value for the height of the antiformal stack. The measured height and length from the sections were plotted against the amount of shortening for comparison with similar plots in the models. The plot shows that the antiformal stack grows in length significantly with time whereas its height remains almost constant (Fig. 5). Similar to plots of model shortened above a low-friction décollement, the height of the antiformal stack in Sulaiman fold belt reaches its maximum sooner than in models with high-basal friction (compare Figs. 4a and 5).

4.2. Layer parallel compaction

Koyi (1988) and Koyi et al. (2003) used dip sections in models shortened from one end to demonstrate that cross-sectional area loss and bed-length change, caused by penetrative strain, depend on basal friction, amount of bulk shortening and the rheological properties of the deformed layers. The models presented here are used to illustrate how penetrative strain depends on the décollement dip. We measured the area in six dip sections from two models deformed by the same amount of bulk shortening. One of the models had a horizontal décollement and the other had a décollement dipping 5° toward the hinterland. We then compared the cross-sectional area between the final and initial stages. The cross-sectional area was measured assuming plain strain (no gain or loss of sand grains and intergrain area in the profiles). In the same profiles, the length of a layer, at equivalent stratigraphic level, was measured and compared with its initial length (Fig. 2). Bed-length was used to calculate the amount of layer-parallel compaction (LPC), which is equivalent to layer-parallel shortening in nature. The source of error in these measurements could be due to sections not having been vertical or exactly parallel to the shortening direction. To overcome this uncertainty, bed-length and areas were measured in three profiles in each model. During this exercise, the difference in measurement of area loss ranged between 0.3 and 0.5%. Another source of error is that during bed-length measurements, it has not been possible to measure those parts of the layers that were distributed by shearing along fault zones. This means that our bed-length calculations give a maximum estimate of LPC.

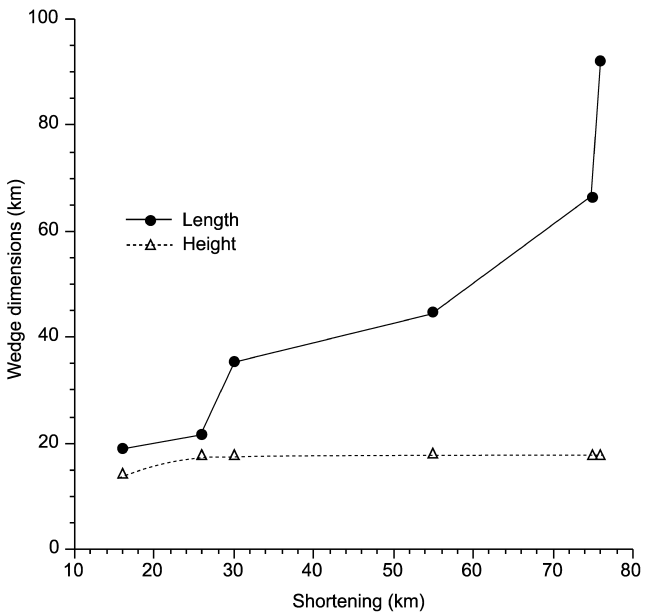

Fig. 5. Height versus length plot of the antiformal stacks in the Sulaiman fold belt in Pakistan as determined from balanced restored sections of Jadoon et al. (1992). Note that, similar to plots of model wedges shortened above a low-friction décollement, length of the antiformal stack increases, whereas its height is nearly constant with progressive shortening.

Analysis of the model profiles show that the models undergo different amounts of area loss depending on their décollement dip; the model with higher décollement dip underwent more area loss (Fig. 2). This area loss is accommodated by lateral compaction of the sand pack and reduction of porosity between the sand grains. Effectively, the area loss measured in the profiles reflects the porosity reduction in the sand pack. In nature, such area loss is manifested by formation of cleavage, and stylolites and bulk porosity reduction (Koyi et al., 2003).

Similar conclusions are applicable for bed-length change; layer parallel compaction (LPC) increases with increasing décollement dip (Fig. 2). These results suggest that as the décollement dip increases, the models accommodate a greater amount of the shortening by lateral compaction in the form of area loss and layer-parallel thickening rather than propagation of the basal décollement. Applied to nature, model results suggest that, other parameters being equal, fold-thrust belts shortened above a steeply dipping décollement shorten by a larger proportion of penetrative strain than fold-thrust belts shortened above a gentler décollement.

4.3. Number of imbricate sheets

The style of deformation in thin-skinned fold and thrust belts is critically dependent upon the resistance to sliding along the detachment between the mass of deforming sediments and the underlying rocks (Davis and Engelder, 1985). The number of imbricates forming depends on the mechanical properties of the shortened layers and on the basal friction. Our models show that basal friction and slope

govern the spacing and size of the imbricates formed in the shortened models. Imbricates formed above a high-friction décollement are more numerous, have irregular spacing, and are of different size, whereas those formed above a low-friction décollement are fewer, have relatively regular spacing, and are in general of similar size (Fig. 3). These differences are present regardless of the basal slope. Two models (one with zero slope and the other with 5° slope) shortened above a low friction décollement formed an equal number of imbricates with similar spacing (Fig. 3B). In contrast, wedges formed in two models (one with zero slope and the other with 5° slope) shortened above a high-friction décollement were comprised imbricates with irregular spacing and which were greater in number than in models shortened above a low-friction décollement (Fig. 3). On the other hand, the basal slope affected the relative angle between the décollement and the thrust planes. Where the décollement dipped landward, the angle between the base and forethrusts was higher, whereas this angle was lower in models where the décollement dipped toward the hinterland.

5. Conclusions

Models of loose sand shortened from one end show that décollement dip has a significant influence on geometry and kinematics of the resulting wedge. Models shortened above a hinterland-dipping décollement develop wedges with steeper taper, have more gently-dipping forethrusts, and undergo a higher amount of penetrative strain in the form of area loss and layer-parallel compaction. In general, at the same amount of bulk shortening, the length/height ratio of wedges formed above a décollement dipping towards the hinterland is less than the same ratio of wedges shortened above a horizontal décollement, which in turn is less than that of wedges shortened above a décollement dipping towards the foreland. However, the presence of a low basal friction tends to reduce the effect of décollement dip.

Acknowledgements

We greatly appreciate the thorough and constructive reviews by Prof. James Evans and an anonymous reviewer on this article. Thanks are due to Christopher Talbot for commenting on part of the manuscript. HAK is funded by the Swedish Science Research Council (VR). These experiments were conducted at the Applied Geodynamics Laboratory at University of Texas at Austin.

References

Colletta, B., Letouzey, J., Pinedo, R., Ballard, J.F., Balé, P., 1991. Computerized X-ray tomography analysis of sandbox models: examples of thin-skinned thrust systems. Geology 19, 1063–1067.

Cotton, J., Koyi, H.A., 2000. Modelling of thrust fronts above ductile and frictional décollements; examples from The Salt Range and Potwar Plateau, Pakistan. GSA Bulletin 112, 351–363.

Dahlen, F.A., Suppe, J., Davis, D.M., 1984. Mechanics of fold and-thrust belts and accretionary wedges (continued). Cohesive Coulomb Theory: Journal of Geophysical Research 89, 10087–10101.

Davis, D., Engelder, T., 1985. The role of salt in fold-and-thrust belts. Tectonophysics 119, 67–88.

Davis, D., Suppe, J., Dahlen, F.A., 1983. Mechanics of fold-and-thrust belts and accretionary wedges. Journal of Geophysical Research 88, 1153–1172.

Gutscher, M.-A., Kukowiski, N., Malavieille, J., Lallemand, S., 1996. Cyclical behavior of thrust wedges: insights from high-basal friction sandbox experiments. Geology 24, 135–138.

Hoshino, K., Koide, H., Inami, K., Iwamura, S., Mitsui, S., 1972. Mechanical properties of Japanese Tertiray sedimentary rocks under high confined pressure. Geological Survey of Japan Report 244, 200pp.

Hubbert, M.K., 1937. Theory of scale models as applied to the study of geologic structures. GSA Bulletin 48, 1459–1520.

Jadoon, I.A.K., Lawrence, R.D., Lillie, R.J., 1992. Balanced and retro-deformed geological cross-section from the frontal Sulaiman Lobe, Pakistan: duplex development in thick strata along the western margin of the Indian Plate. In: McClay, K.R., (Ed.), Thrust Tectonics, Chapman and Hall, London, pp. 343–356.

Koyi, H.A., 1988. Experimental modeling of the role of gravity and lateral shortening in the Zagros mountain belt. AAPG Bulletin 72, 1381–1394.

Koyi, H.A., 1995. Mode of internal deformation in sand wedges. Journal of Structural Geology 17, 293–300.

Koyi, H.A., Petersen, K., 1993. The influence of basement faults on the development of salt structures in the Danish Basin. Marine and Petroleum Geology 10, 82–94.

Koyi, H.A., Hessami, K., Teixell, A., 2000. Epicenter distribution and magnitude of earthquakes in fold-thrust belts: insights from sandbox modeling. Geophysical Research Letters 27, 273–276.

Koyi, H.A., Sans, M., Teixell, A., Cotton, J., Zeyen, H., 2003. The significance of penetrative strain in contractional areas. In: McClay, K.R. (Ed.), Thrust Tectonics. American Association of Petroleum Geology Memoire, in press.

Liu, H., McClay, K.R., Powell, D., 1992. Physical models of thrust wedges. In: McClay, K.R., (Ed.), Thrust Tectonics, Chapman and Hall, London, pp. 71–81.

Mariotti, G., Doglioni, C., 2000. The dip of the foreland monocline in the Alps and Appenines. Earth and Planetary Science Letters 181, 191–202.

Mulugeta, G., Koyi, H.A., 1992. Episodic accretion and strain partitioning in a model sand wedge. Tectonophysics 202, 319–333.

Namson, J., 1982. Studies of the structure, stratigraphic record of plate interaction and role of pore-fluid pressure in the active fold and thrust belt of Taiwan and study of manganese deposits form northern California. Doctoral Thesis, Princeton University, Princeton, NJ.

Suppe, J., 1980a. A retrodeformable cross section of northern Taiwan. Proceedings of the Geological Society of China 23, 46–55.

Suppe, J., 1980b. Imbricated structure of Western Foothills Belt, south central Taiwan. Petroleum Geology of Taiwan, 17, 1–16.

Suppe, J., Namson, J., 1979. Fault bend origin of frontal folds of the western Taiwan fold-and-thrust belt. Petroleum Geology of Taiwan, 16. 1–18.

Vendeville, B.C., Cobbold, P.R., Davy, P., Brun, J.P., Choukrone, P., 1987. Physical models of extensional tectonics at various scales. In: Coward, M.P., Dewey, J.F., Hancock, P.L. (Eds.), Continental extensional tectonics. Geological Society Special Publication 28, pp. 95–107.

von Huene, R., 1986. Seismic images of modern convergent margin tectonic structure. AAPG Studies 26, 1–60.

Weijermars, R., Jackson, M.P.A., Vendeville, B.C., 1993. Scaling of salt tectonics. Tectonophysics 217, 143–174.

Willett, S.D., 1992. Dynamic and kinematic growth and change of a Coulomb wedge. In: McClay, K.R., (Ed.), Thrust Tectonics, Chapman and Hall, London, pp. 19–31.